Ternary $H_2SO_4/HNO_3/H_2O$ Optical Constants: New Measurements from Aerosol Spectroscopy under Stratospheric Conditions

M. L. Norman[†] and R. E. Miller*

Department of Chemistry, University of North Carolina, Chapel Hill, North Carolina 27599-3290

D. R. Worsnop

Center for Aerosol and Cloud Chemistry, Aerodyne Research, Inc., Billerica, Massachusetts 01821-3976

Received: November 12, 2001; In Final Form: April 19, 2002

We present here the first measurements of the infrared complex refractive indices for supercooled ternary solutions of H_2SO_4, HNO_3, and H_2O under stratospheric conditions. The data sets were retrieved directly from the infrared extinction spectra of laboratory-generated aerosols. Comparisons of these results with a previously reported empirical mixing rule model[1] reveal significant differences, which we trace to errors in the binary acid/water thin film refractive indices used in the model. In addition, the model does not properly account for the concentrations of ionic and neutral species in the ternary solutions. The experimentally determined optical constants reported here will be useful for determining polar stratospheric cloud aerosol properties from infrared spectroscopic remote sensing measurements.

Introduction

It is now well-established that polar stratospheric clouds (PSCs) play a crucial role in the annual depletion of the polar ozone layer.[2,3] Although the chemical and physical processes associated with the formation of the ozone hole are qualitatively understood, there is continuing debate over the composition and phase of the aerosols that make up these clouds. Considerable evidence now exists to suggest that PSCs consist of supercooled ternary solutions (STSs) of H_2SO_4, HNO_3, and H_2O, formed as nitric acid vapor condenses onto background sulfate aerosols during the polar winter.[4,5] Satellite- and aircraft-based infrared remote sensing measurements are employed to elucidate PSC properties such as composition, phase, and particle number density. These measurements require the absorption and scattering properties of PSC aerosols to be well-characterized. In particular, the infrared complex refractive indices (optical constants) must be determined from laboratory experiments over the appropriate range of stratospheric conditions. This aspect of the problem is addressed in the present paper.

Although data sets have been published for the binary H_2SO_4/H_2O[6−12] and HNO_3/H_2O[7,13−18] systems over a wide range of solution compositions and temperatures, only one experimental data set exists for the ternary $H_2SO_4/HNO_3/H_2O$ system, that of Adams and Downing[19] for a 75 wt % H_2SO_4, 10 wt % HNO_3, and 15 wt % H_2O solution at room temperature. This lack of data is in part related to the difficulties associated with the quantitative determination of compositions of the thin film or aerosol samples that are often used in the optical constant measurements, a point we will address specifically here. Given that the optical constants of these acidic solutions depend on both composition and temperature, a large number of data sets are required to fully explore this dependence. The focus of the present study will be on those regions of the ternary phase diagram that correspond most closely to the polar stratosphere.

Biermann and co-workers[1] recently published an empirical model for calculating the infrared refractive indices of ternary $H_2SO_4/HNO_3/H_2O$ solutions using linear combinations of the binary H_2SO_4/H_2O and HNO_3/H_2O optical constants. Imaginary refractive indices for the ternary solutions (k_T) as a function of frequency, temperature, and weight percent sulfuric acid (W_S) and nitric acid (W_N) are calculated using the expression

$$k_T(\nu,T,W_S,W_N) = \frac{W_S}{W_S + W_N} k_S{}^b(\nu,T,W_S{}^b) + \frac{W_N}{W_S + W_N} k_N{}^b(\nu,T,W_N{}^b) \quad (1)$$

Here, $k_S{}^b$ and $k_N{}^b$ are the imaginary indices of binary acid/water solutions corresponding to weight percentages of $W_S{}^b$ and $W_N{}^b$, respectively, given by

$$W_S{}^b = W_N{}^b = W_S + W_N \quad (2)$$

The model employs binary data sets that the authors determined from thin film absorption spectra collected over a wide range of temperatures and compositions,[1] which are interpolated for calculations at intermediate conditions. The underlying assumption in this empirical model is that the water activities in the binary solutions are the same as those in a ternary solution having the same total acid concentration. This assumption is supported by an ion interaction model that was first presented by Luo et al.,[20] which seems to be valid for calculating ternary solution refractive indices in the ultraviolet (where $k \approx 0$), for solutions having total acid concentrations of 5−70 wt %. Biermann et al. claim that the mixing rule is valid in the infrared as well for ternary solutions in which $H_2SO_4 \leq 80$ wt %, $HNO_3 \leq 50$ wt %, and $183 \leq T \leq 293$ K. The obvious attraction of the model is that it permits the calculation of optical constants for a wide range of conditions using a limited amount of experimental data on only the binary systems. Although the

* To whom correspondence should be addressed.
[†] Present address: SensIR Technologies, Danbury, CT 06810.

10.1021/jp014138v CCC: $22.00
Published on Web 05/31/2002

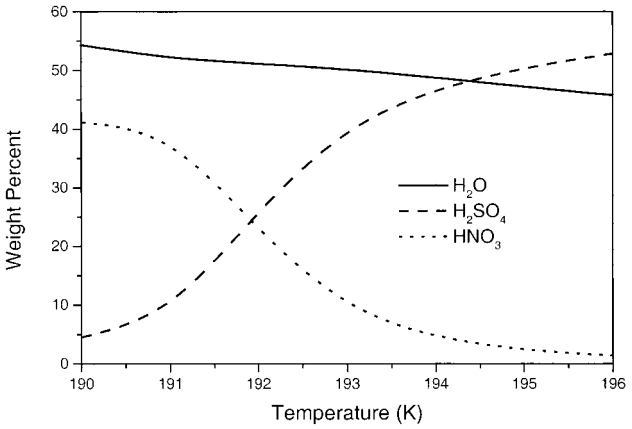

Figure 1. Compositions, based upon the Carslaw et al. thermodynamic model, of ternary solution aerosols under polar stratospheric conditions. Input parameters used for this calculation were 5 ppmv H_2O, 0.5 ppbv H_2SO_4, and 10 ppbv HNO_3 at 50 mbar total pressure.

model was tested by comparing its results with infrared spectra of ternary solutions, the lack of corresponding optical constants has not yet allowed for a quantitative test of the method.

The focus of the present study is on determining complex refractive indices for STSs directly from the spectra of laboratory-generated aerosols in the temperature and composition range of stratospheric interest. Given the average mixing ratios that have been measured for sulfuric acid, nitric acid, and water in the stratosphere,[5] thermodynamic models predict that "pure" STS aerosols at polar stratospheric temperatures may have compositions of approximately 40−50 wt % H_2O with the remaining 50−60 wt % consisting of H_2SO_4 and HNO_3 [21,22] in the ratios shown in Figure 1. It is important to note here that in previous studies of binary mixtures, we have shown that the temperature and composition dependence of acid/water optical constants can be significant.[12] However, because the temperature range of interest here is rather narrow, we expect these temperature effects to be weak and the composition dependence of the optical constants to be more significant. We therefore chose to carry out all of the present measurements at a single temperature (220 K), slightly higher than that of the polar stratosphere, to avoid potential problems associated with freezing of the aerosols. This also ensured that the equilibrium vapor pressures of the surrounding vapors were high enough to be measured using our tunable diode laser system, a prerequisite for determining the compositions of the aerosols (as discussed below). The optical constants determined here correspond to $H_2SO_4/HNO_3/H_2O$ ternary solutions of approximately 45 wt % H_2O. Although these new data sets agree qualitatively with the empirically calculated results of Biermann et al.,[1] there are some significant differences. We have traced these differences to errors in the binary acid/water thin film refractive indices employed in the model and to the fact that the model does not explicitly consider the effects of acid solute dissociation on the ternary solution optical properties.

Experiment

Ternary Aerosol Nucleation and Spectroscopy. All of the data presented here were collected in our aerosol flow cell, shown in Figure 2 and discussed in detail previously.[12] The cell has six independent cooling sections to allow for separate control (to ±1 K) of the aerosol nucleation and observation temperatures. Ternary $H_2SO_4/HNO_3/H_2O$ droplets were produced by first generating a stream of concentrated H_2SO_4 aerosols entrained in a helium carrier gas using a glass vaporizer.[12] The median size of the particles produced was varied by changing the temperature of the sulfuric acid in the vaporizer and the flow rate of the helium carrier gas. The resulting particles were then diluted by mixing the flow with humidified helium in a heated glass mixing bulb. A third helium gas stream was saturated with a 70 wt % nitric acid solution and combined with

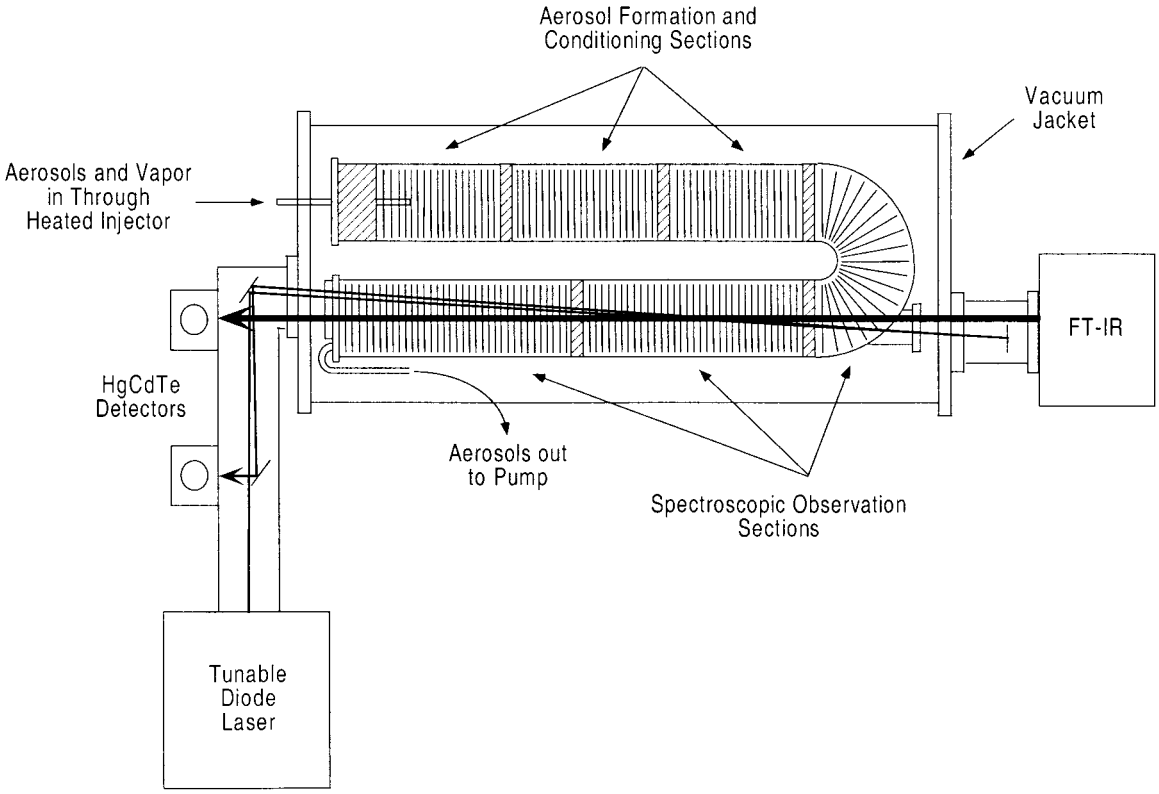

Figure 2. A schematic diagram of the multisectioned, temperature-controlled aerosol flow cell.

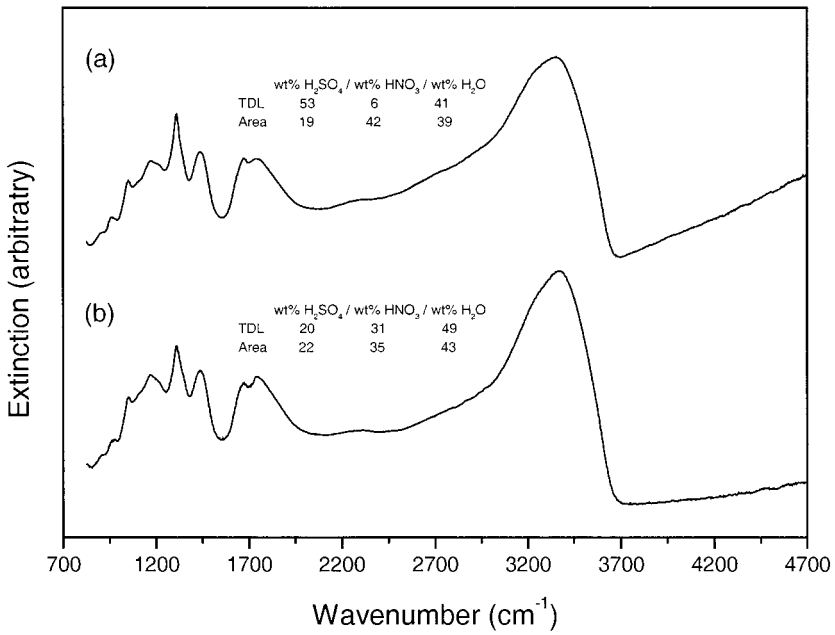

Figure 3. Small-particle FT-IR spectrum (a) of a mixture of binary H_2SO_4/H_2O, binary HNO_3/H_2O, and ternary aerosols (offset for clarity) with measured vapor pressures of $p_{water} = 3.8 \times 10^{-3}$ Torr and $p_{nitric} = 1.4 \times 10^{-4}$ Torr and (b) of ternary $H_2SO_4/HNO_3/H_2O$ aerosols with measured vapor pressures of $p_{water} = 9.3 \times 10^{-3}$ Torr and $p_{nitric} = 7.0 \times 10^{-5}$ Torr. When the binary particles are present, the compositions determined from the corresponding vapor pressures are inconsistent with the integration method of Anthony et al., while for panel b, the two methods give qualitatively similar results.

the H_2SO_4/H_2O aerosol stream. Upon injection of this mixture into the first section of the flow cell, held at 240 K, the nitric acid vapor condensed onto the sulfate aerosols to form the ternary solutions. The flow rates of the various gas streams were used to control the compositions of the resulting particles. The upper half of the aerosol flow cell was set so that the temperature decreased along its length, 240 K at the input to 220 K at the bend. The entire lower half of the flow cell was maintained at 220 K. As indicated in the figure, the output from a Bomem DA3.02 Fourier transform infrared (FT-IR) spectrometer was directed through the lower half of the flow cell. Spectra were recorded from 825 to 5000 cm^{-1} at a resolution of 4 cm^{-1}. The total gas flow through the cell ranged from 1 to 3 standard liters per minute, with total cell pressures of 80−150 Torr. This corresponded to an average residence time of particles in the cell of approximately 45 s.

Although the method described above is a convenient approach for making aerosol particles of widely different compositions, useful data can only be obtained if we can accurately determine these compositions. In particular, because these particles are volatile, the compositions must be determined in the region of the flow cell where the FT-IR analysis occurs. In a study of ternary particle crystallization, Anthony et al.[23] employed an empirical approach in which integrated absorbances over specific regions of their FT-IR aerosol spectra were calibrated against those of room temperature thin films. This approach is certainly easy to implement and the authors cited reasonable errors, ±3 wt % for HNO_3 and H_2SO_4 and ±6 wt % for H_2O. This approach obviously does not account for any temperature dependence in the absorption bands and fails when a significant amount of light scattering is present in an aerosol spectrum of the type considered here. These problems were avoided in the present study by making use of a high-resolution tunable diode laser (TDL) spectrometer to measure the vapor pressures of water and nitric acid in equilibrium with the particles. The ternary solution concentrations were determined by iteratively solving the Carslaw et al.[24] thermodynamic model, given the measured vapor pressures. This iterative process yields concentrations with estimated errors of ±2 wt % H_2SO_4, ±2 wt % HNO_3, and ±1 wt % H_2O, primarily related to small uncertainties in the cell temperature. It should be noted that, given the average particle residence time of 45 s (discussed above) and typical median particle sizes of <1 μm (discussed below), the assumption of ternary aerosol/vapor equilibrium is valid on the time scale of these experiments. Indeed, the approach of determining aerosol compositions from TDL vapor pressure measurements has been successfully applied in our previous studies of binary H_2SO_4/H_2O[12] and HNO_3/H_2O[18] aerosols.

As mentioned above, the TDL approach for the in situ determination of the particle compositions is limited by the minimum detectable vapor pressure. In the present study, HNO_3 was the limiting species, because the lowest measurable nitric acid vapor pressure of 8×10^{-5} Torr could not be detected below 220 K. In fact, the vapor pressures of HNO_3 employed in this study were greater than those typically measured for HNO_3 in the stratosphere.[5] However, the aerosol compositions (in terms of wt % acid) that we achieved by varying the partial pressures of water and nitric acid isothermally at 220 K were directly relevant to upper atmospheric aerosol concentrations (see Figure 1). Although 220 K is at the high end of the stratospherically relevant temperature range,[25] we again expect that the temperature dependence of the optical constants will be unimportant over the range 190−220 K at these total acid concentrations upon the basis of our previous studies of the binary acid/water systems.[12,18]

A critically important consideration in this study is that ternary solution aerosols be produced exclusively such that no binary H_2SO_4/H_2O or HNO_3/H_2O aerosols are nucleated. As noted by Anthony et al.,[23] the latter would result in partial pressures of H_2O and HNO_3 that are very different from that of pure ternary aerosols, which would invalidate our composition determinations. The effect of nucleating binary aerosols is illustrated in Figure 3, in which we attempted to nucleate ternary aerosols with the entire flow cell set at 220 K. At this temperature, we know empirically[18] that binary nitric acid/water particles can

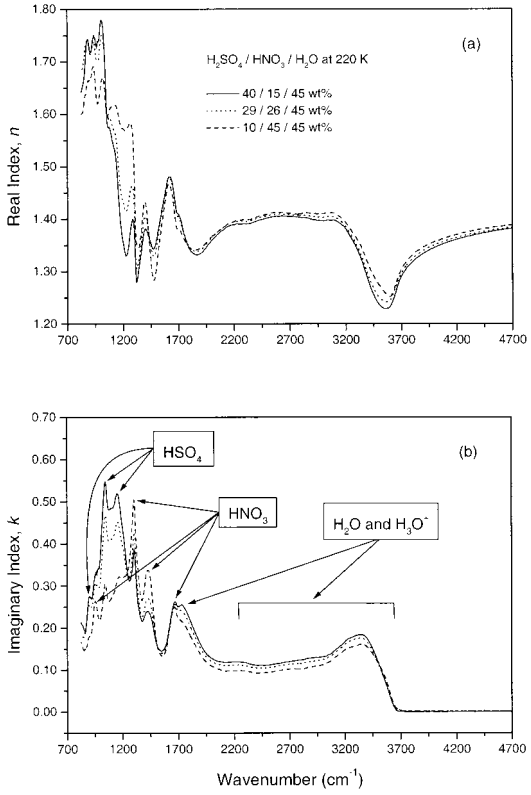

Figure 4. Selected real (a) and imaginary (b) refractive indices for ternary aerosols determined at 220 K and showing the smooth variation with composition.

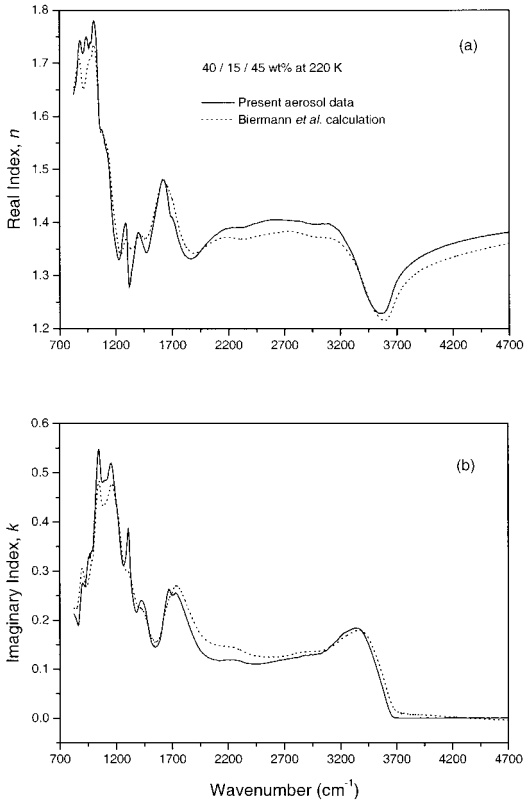

Figure 5. Comparison of the real (a) and imaginary (b) refractive indices for 40 wt % H_2SO_4/15 wt % HNO_3/45 wt % H_2O at 220 K determined from the present ternary aerosol spectra (solid line) and calculated using the mixing rule of Biermann et al. (dotted line).

nucleate. In this scenario, the resulting vapor pressures gave compositions, based upon the assumption that only ternary aerosols were present, that were very inconsistent with those obtained from the area method calculations of Anthony et al. for weakly scattering aerosols. Figure 3a shows an FT-IR spectrum recorded under these conditions. Although the coexistence of binary and ternary particles is nonequilibrium, the time scale for the binary particles to evaporate and for the vapor to be incorporated into the ternary particles is much longer than the residence time of the particles in the cell.[23] Thus, once these binary nitric acid/water particles form, they remain for the entire observation time. The only way to avoid this nonequilibrium condition is to make sure that the binary particles never nucleate. This problem is overcome by imposing a temperature gradient in the upper sections of the cell (from 240 to 220 K) so that the nitric acid/water vapor never becomes supersaturated. Under these conditions, the only possibility is for the nitric acid and water to condense on the preformed sulfuric acid aerosols, making the ternary particles. This simple change resulted in the spectrum shown in Figure 3b, in which the measured vapor pressures gave compositions in qualitative agreement with the area method. We note that in subsequent experiments, in which we varied the temperature of the first section from 230 to 260 K, similar results were obtained. Thus, we could be confident that only ternary droplets were formed in our experiments and the measured vapor pressures provided accurate solution compositions using an equilibrium model.[24] These observations illustrate the need for carefully nucleating the ternary aerosols such that the aerosol/vapor equilibrium is not taken for granted.

Optical Constant Calculations. Having demonstrated our ability to produce ternary aerosols over a range of compositions, we will briefly describe the methods used in our laboratory for determining the frequency-dependent real and imaginary components of the corresponding refractive indices directly from the FT-IR extinction spectra. This was accomplished using the iterative fitting procedure that we have reported previously for several other systems.[11,16,17,26] The method begins with an estimate of the imaginary component of the refractive index ($k(\nu)$), obtained from an FT-IR spectrum of small particles (<0.1 μm median radius) that, to a first approximation, do not scatter infrared radiation.[27] In some cases, we were unable to form small enough particles, so the scattering component had to be approximated and subtracted from the aerosol spectra. This method has been employed previously and is discussed in detail elsewhere.[18] Note that in the first iteration it is necessary to estimate the absolute scaling factor for $k(\nu)$ because the absolute number density of the particles in the cell is not known initially. This initial guess is refined in the iterative procedure discussed below.

With $k(\nu)$ estimated, the corresponding real component ($n(\nu)$) is calculated using a subtractive Kramers−Kronig transform.[27] This calculation requires that an "anchor point" value of the real refractive index be known at one frequency at which no absorption features are present but that is within the integration limits. We therefore estimated n at 5000 cm^{-1} using the calculated values of Luo et al.[20] Truncation of the data sets introduces errors in the Kramers−Kronig transform, particularly at the low-frequency end of the spectrum. In previous studies, we have shown that these errors can be minimized by extending the imaginary indices to lower frequencies using room-temperature data for similar systems.[12,17,18] In the present study, we estimated the imaginary indices from 825 to 400 cm^{-1} by summing together room-temperature binary data[9,14] of approximately the same total acid composition of the ternary solution and scaling the result to match k at 825 cm^{-1}. However, the data sets reported here only include the points above 825 cm^{-1}.

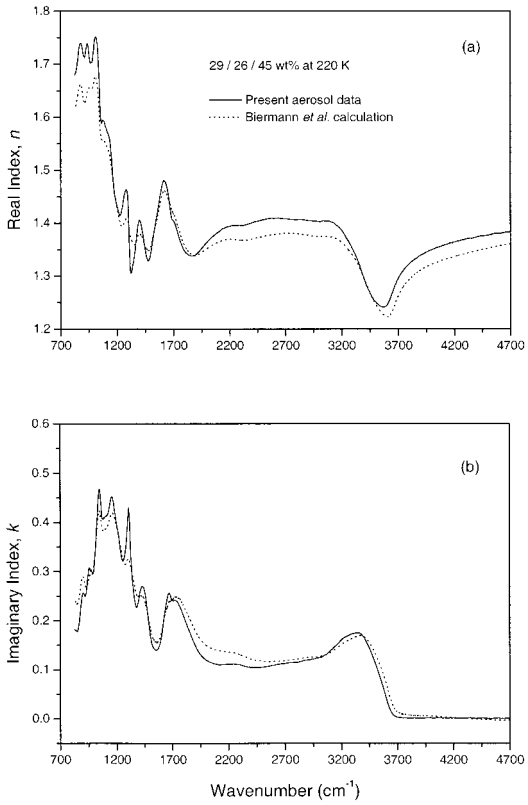

Figure 6. Comparison of the real (a) and imaginary (b) refractive indices for 29 wt % H_2SO_4/26 wt % HNO_3/45 wt % H_2O at 220 K determined from the present ternary aerosol spectra (solid line) and calculated using the mixing rule of Biermann et al. (dotted line).

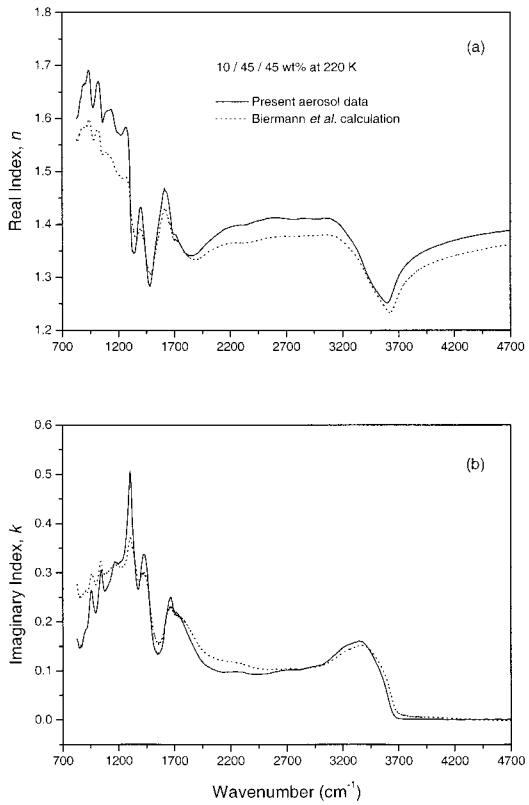

Figure 7. Comparison of the real (a) and imaginary (b) refractive indices for 10 wt % H_2SO_4/45 wt % HNO_3/45 wt % H_2O at 220 K determined from the present ternary aerosol spectra (solid line) and calculated using the mixing rule of Biermann et al. (dotted line).

Starting from this estimated set of real and imaginary complex refractive indices, Mie scattering calculations were used to simulate a spectrum of large particles ($>0.5\ \mu$m median radius), which exhibit strong scattering. In these cases, the spectra show structure that arises from the interplay between the scattering and absorption contributions[26] such that they are sensitive to both the real and imaginary components of the refractive indices. This calculation is performed by averaging over a log-normal particle size distribution defined by a median radius, r_{med}, and width, σ. The calculated spectrum is then iteratively fit to the experimental data by adjusting the parameters associated with the size distribution and the $k(\nu)$ scaling factor. We have shown previously that for particle spectra exhibiting strong scattering components, the calculation converges to a unique solution for the optical constants.[26] We have estimated that the relative error in the $k(\nu)$ and $n(\nu)$ data sets generated by this method is $\pm 3\%$ and the absolute error in k is approximately ± 0.005 index units.[11]

Results and Discussion

Composition Trends in the Refractive Indices. From a database of aerosol extinction spectra recorded in the manner discussed above, we generated six frequency-dependent complex refractive index sets covering the mid-infrared spectral region from 825 to 5000 cm^{-1}. The 220 K ternary aerosols all had compositions of approximately 45 wt % H_2O and varying amounts H_2SO_4 and HNO_3. In what follows, we will refer to the aerosol concentrations as *s*/*n*/*w* wt %, where s = wt % H_2SO_4, n = wt % HNO_3, and w = wt % H_2O. The optical constants obtained from these spectra are shown in Figure 4 for three of the compositions. In all cases, the imaginary indices exhibit strong absorption features in the region from 800 to 1800 cm^{-1}. As noted by Anthony et al.,[23] none of the features are unique to the ternary solutions, but rather all can be assigned to the ionic and molecular absorption bands of the constituent solutes and solvent. In Figure 4b, the bands at 890, 1050, and 1180 cm^{-1} are assigned to the HSO_4^- ion,[6] and the bands at 949, 1304, and 1429 cm^{-1} are due to the HNO_3 molecule.[14] The band near 1700 cm^{-1} contains overlapping features from the ν_2 mode of H_2O at 1640 cm^{-1}, the ν_2 mode of HNO_3 at 1672 cm^{-1}, and the ν_4 mode of H_3O^+ at 1742 cm^{-1}.[14] The signature features of the SO_4^{-2} ion at 1105 cm^{-1} and the NO_3^- ion at 1040 cm^{-1}, which were observed in binary acid/water systems, are not observed here, indicating that the bisulfate ion and the nitric acid molecule are the principle solute species at these ternary solution concentrations.

It is evident from Figure 4b that the bands associated with the acid absorption features in the imaginary indices (appearing at the low-frequency part of the spectrum) vary smoothly with acid concentration. In turn, the intensity of the broad O−H stretch band of the water solvent (centered near 3300 cm^{-1} [14]) also changes, a somewhat surprising result given that the data sets all correspond to the same wt % water. It is nevertheless clear that the intensity of the O−H feature decreases with the concentration of the sulfuric acid. This effect can be attributed to the stronger hydrogen bonding between water solvent and the HSO_4^- ion, compared to that with the HNO_3 molecule. This observation is consistent with what we have observed previously in the binary H_2SO_4/H_2O $k(\nu)$ data.[18] With these new data sets in hand, we can now make comparisons with the optical constants modeled using the Biermann et al.[1] mixing rule.

Comparisons to Model Calculations. We have already presented the mathematical treatments and underlying assumptions of the Biermann et al.[1] model for calculating $H_2SO_4/HNO_3/H_2O$ infrared refractive indices. In Figures 5−7, we make

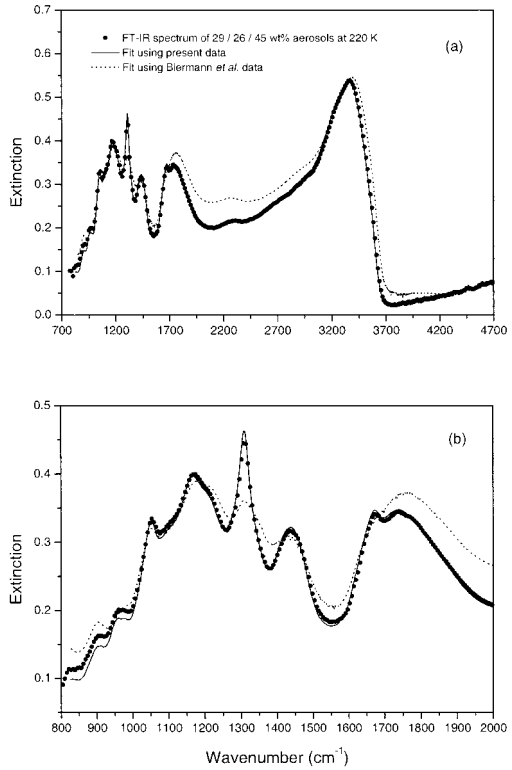

Figure 8. Mie simulations (a) of 29 wt % H_2SO_4/26 wt % HNO_3/45 wt % H_2O aerosols at 220 K. The present optical constants (solid line) fit the spectrum with $r_{med} = 0.013$ μm and $\sigma = 0.092$, while the Biermann et al. results (dotted line) give $r_{med} = 0.015$ μm and $\sigma = 0.090$. Panel b shows an expanded view of the acid absorption band region.

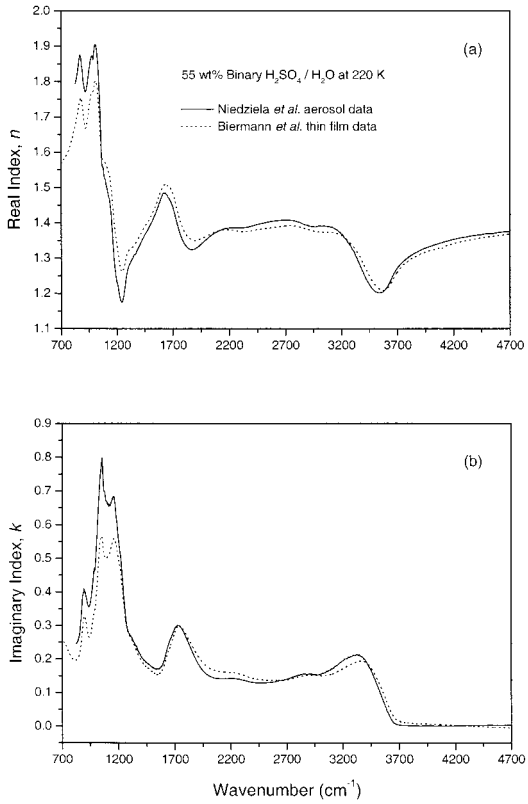

Figure 9. Comparison of the real (a) and imaginary (b) refractive indices for 55 wt % H_2SO_4/H_2O at 220 K determined by Niedziela et al. (solid line) and by Biermann et al. (dotted line).

comparisons between the model calculations and the three data sets introduced above. Qualitatively, the agreement is quite good, considering that very different approaches were used in the two laboratories. Nevertheless, there are some significant differences, particularly in the solute bands at the lower frequencies. For instance, the two bisulfate bands near 1100 cm^{-1} have higher intensity in the present data sets for all concentrations. Even more striking are the differences between the HNO_3 bands at 1304, 1429, and 1672 cm^{-1}. In the 40/15/45 and 29/26/45 wt % cases, these bands are nearly indistinguishable in the Biermann et al. data sets. In addition, the shape of the 1700 cm^{-1} band, in which HNO_3, H_2O, and H_3O^+ features overlap, is much different in the Biermann et al. data at these concentrations. For the 10/45/45 wt % case, the HNO_3 features are noticeable in the Biermann et al. optical constants, but the strongest band at 1304 cm^{-1} is much stronger in the data set obtained here. At the higher frequencies, at which $k(\nu)$ is dominated by water solvent absorption, the agreement is rather good at all concentrations, although the O−H stretch in the present data is slightly red-shifted with respect to the Biermann et al. data.

Another peculiarity is the differences in $n(\nu)$ at the highest frequencies, at which there are no absorption features, given that the anchor point in the real refractive indices (used in the subtractive Kramers−Kronig analyses) were obtained from Luo et al.[20] in both cases. Nevertheless, because the Biermann et al. ternary optical constants were obtained by interpolation of their binary acid/water data sets, for which $n(\nu)$ was originally produced using n at 12 820 cm^{-1} as the anchor point,[1] the errors in the Biermann et al. model likely result from interpolating the real refractive indices over composition and temperature. Figure 8 shows an example of how these differences in $n(\nu)$ and $k(\nu)$ influence the Mie scattering simulation of a ternary aerosol spectrum. Note that this is a spectrum of slightly scattering aerosols that was not used in the original retrieval of the present optical constants. Although the two sets of optical constants give similar particle size distributions, the Biermann et al. results do not reproduce all of the features in the aerosol spectra, particularly at the lower frequencies. Similar differences were observed in the Mie scattering analyses of the FT-IR spectra at the other ternary aerosol compositions.

In an attempt to understand the source of the differences between these two data sets, we considered first the possibility that they arise from errors in the composition determinations in either of the experiments. Indeed, at first sight, the differences between the acid solute band intensities suggest that the present data sets correspond to more concentrated solutions relative to the Biermann et al. data. However, we were unable to get better agreement by adjusting the relative acid concentrations in the Biermann et al. model. Our conclusion is that the differences cannot be explained by simple errors in the aerosol composition analysis.

We now consider the model of Biermann et al.[1] in somewhat more detail. In particular, we begin by examining the binary refractive index data used as input to this model. This could certainly be an issue, given that Biermann et al. already noted significant differences between their 50 wt % binary H_2SO_4/H_2O optical constants and those of Niedziela et al.[12] and Tisdale et al.,[10] particularly in the 1100 cm^{-1} bisulfate band. In addition, the most concentrated nitric acid thin film data published by Biermann et al. is 50 wt %, so the 55 wt % HNO_3 needed for the present study represents an extrapolation (according to eq 2). Problems were also encountered in the model results due to errors in the data files for 50 wt % HNO_3 at 223 and 233 K originally published by Biermann et al. Consequently, it was

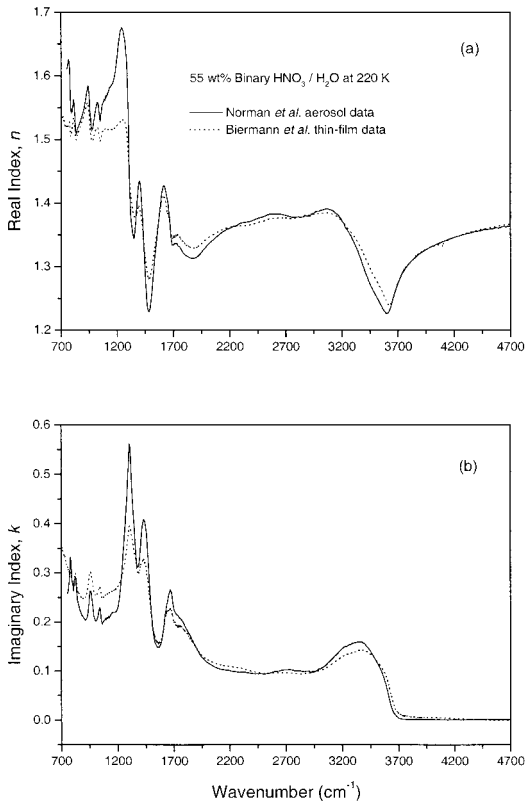

Figure 10. Comparison of the real (a) and imaginary (b) refractive indices for 55 wt % HNO_3/H_2O at 220 K determined by Norman et al. (solid line) and by Biermann et al. (dotted line).

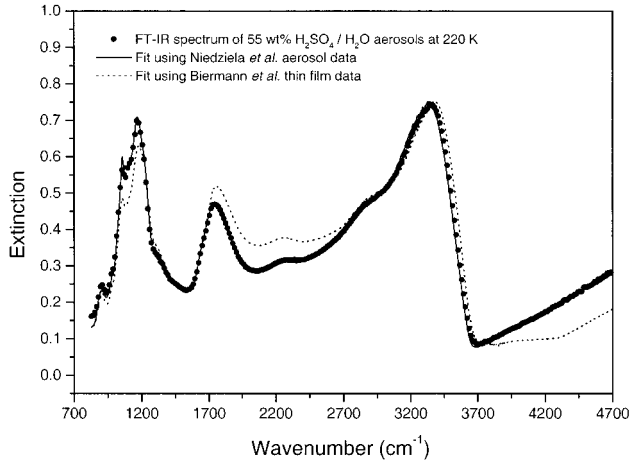

Figure 11. Mie simulations (●) of 55 wt % H_2SO_4/H_2O aerosols at 220 K. The binary aerosol optical constants (Niedziela et al., solid line) give a good fit to the spectrum with $r_{med} = 0.12$ μm and $\sigma = 0.54$, while the Biermann et al. data (dotted line) result in a poorer fit with $r_{med} = 0.11$ μm and $\sigma = 0.50$.

necessary to use their optical constants for 50 wt % HNO_3 at 253 K for the mixing rule model calculations presented here [B. P. Luo, personal communication, 2000].

Figure 9 shows a comparison between the Niedziela et al.[12] optical constants (obtained using the same method employed here for the ternary aerosols) for 55 wt % H_2SO_4/H_2O at 220 K and those of Biermann et al.[1] for the same conditions. The imaginary refractive indices generally agree, but the bisulfate bands near 1100 cm^{-1} are much more intense in the aerosol data set. Figure 10 shows a comparison of the Norman et al.[18] optical constants for 55 wt % HNO_3/H_2O at 220 K to the Biermann et al. 50 wt % HNO_3/H_2O data. Here again, there is

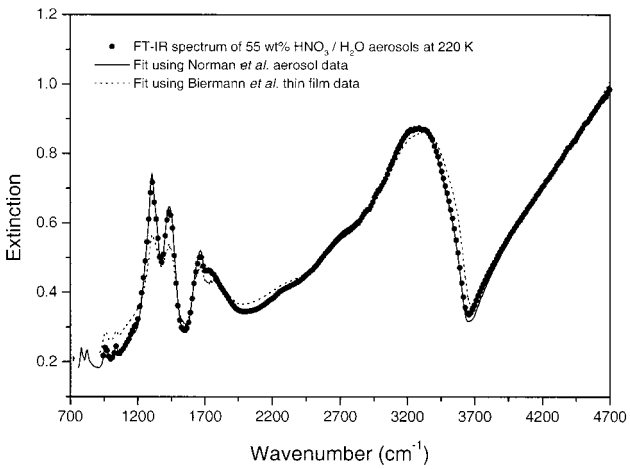

Figure 12. Mie simulations (●) of 55 wt % HNO_3/H_2O aerosols at 220 K. The binary aerosol optical constants (Norman et al., solid line) give a good fit to the spectrum with $r_{med} = 0.55$ μm and $\sigma = 0.34$, while the Biermann et al. data (dotted line) result in a poorer fit with $r_{med} = 0.63$ μm and $\sigma = 0.23$.

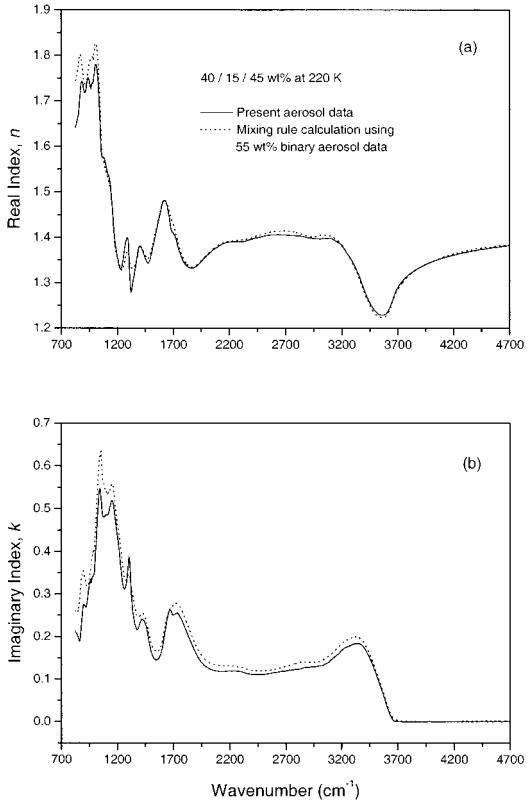

Figure 13. Comparison of the real (a) and imaginary (b) refractive indices for 40 wt % H_2SO_4/15 wt % HNO_3/45 wt % H_2O at 220 K determined from ternary aerosol spectra (solid line) and calculated by employing the binary acid/water aerosol optical constants in the mixing rule model of Biermann et al. (dotted line).

qualitatively good agreement between the imaginary indices, but the nitric acid features near 1300 cm^{-1} are much more intense in the aerosol data sets than in those obtained from the thin film study. It is evident in both figures that $k(\nu)$ in the region of the O−H stretch (near 3300 cm^{-1}) is slightly more intense and red-shifted in the aerosol data, in comparison to the thin film measurement. Figures 11 and 12 depict Mie simulations of 55 wt % binary acid/water aerosol spectra collected in the aerosol flow cell, using the two sets of optical constants. Again, neither of these aerosol spectra was used in

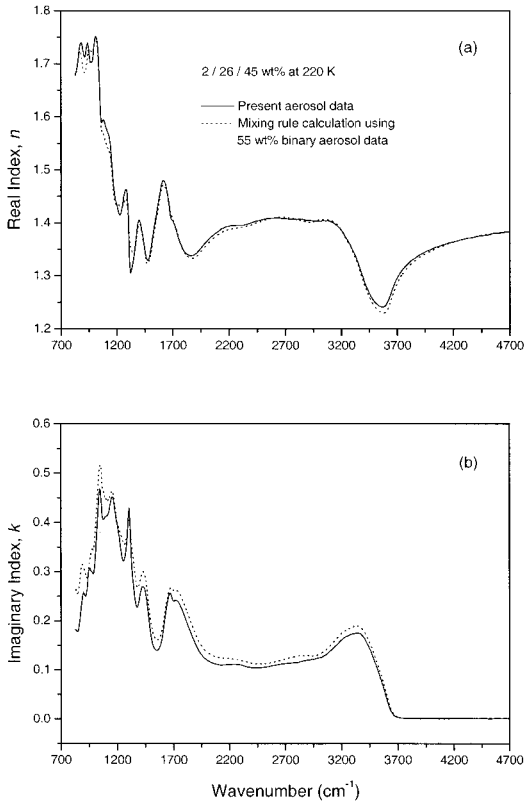

Figure 14. Comparison of the real (a) and imaginary (b) refractive indices for 29 wt % H_2SO_4/26 wt % HNO_3/45 wt % H_2O at 220 K determined from ternary aerosol spectra (solid line) and calculated by employing the binary acid/water aerosol optical constants in the mixing rule model of Biermann et al. (dotted line).

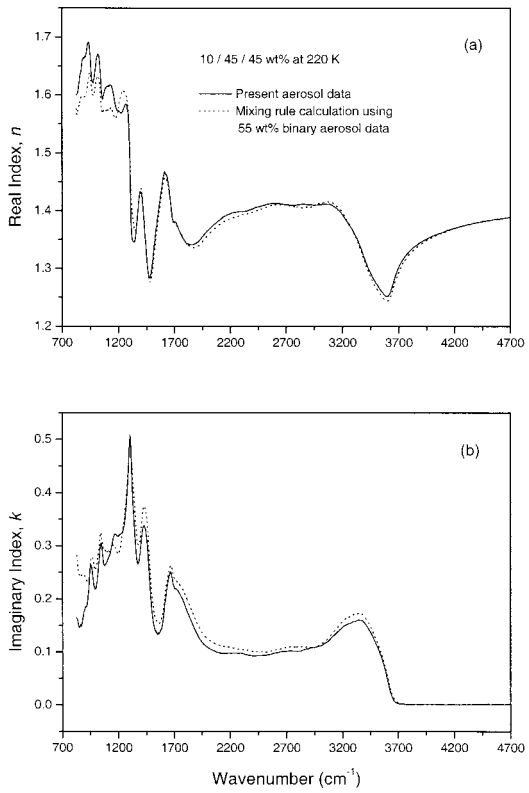

Figure 15. Comparison of the real (a) and imaginary (b) refractive indices for 10 wt % H_2SO_4/45 wt % HNO_3/45 wt % H_2O at 220 K determined from ternary aerosol spectra (solid line) and calculated by employing the binary acid/water aerosol optical constants in the mixing rule model of Biermann et al. (dotted line).

the mathematical retrievals of the optical constants. As expected, the data set obtained from the aerosol spectra gives an excellent fit to this spectrum. The quality of the fit obtained from the Biermann et al. data is somewhat poorer. In trying to access which sets of data are more reliable, we wish to point out that the aerosol method presented here has been benchmarked against a number of well-established data sets, including those of bulk water ice. This gives us confidence to suggest that the source of the differences illustrated here is at least partially a problem with the Biermann et al. binary data sets.

In light of these differences in the binary data sets, we also used their mixing rule with the binary data sets of Niedziela et al.[12] and Norman et al.[18] As shown in Figures 13−15, the resulting refractive indices give better agreement with the present aerosol data sets compared to those in Figures 5−7. Nevertheless, there are still some differences in the 40/15/45 and 29/26/45 wt % cases, particularly in the bisulfate bands near 1100 cm^{-1}. Although the agreement is quite good for the HNO_3 features for all concentrations, there are some differences in the 1304 and 1429 cm^{-1} band intensities. In addition, the shape of the 1700 cm^{-1} feature in the modeled data is somewhat different from that in the experimental ternary spectrum, which was also the case for the Biermann et al. binary optical constants. The most significant improvement is in the shape of the modeled $k_T(\nu)$ data in the solvent O−H stretching region (1750−3500 cm^{-1}), which is more consistent with the present data. The origin of the small offset in $k_T(\nu)$ is not completely understood but is probably the result of the propagation of small errors in the $k(\nu)$-scaling factors used in deriving the binary aerosol optical constants from FT-IR spectra.

Conclusions

We have presented the first measurements of the ternary $H_2SO_4/HNO_3/H_2O$ infrared optical constants derived from the extinction spectra of aerosols studied under stratospherically relevant conditions. The data sets are available from the authors or can be downloaded by anonymous file transfer protocol from our site, ftp://frenchie.chem.unc.edu. Comparisons between the present results and those of Biermann et al.[1] show systematic differences that we suggest partially arise from small errors in their binary data sets. We find that their mixing rule gives much better agreement with the present ternary data sets if the binary optical constants obtained from aerosol studies are used. Nevertheless, differences still remain that we feel are related to deficiencies in the simple mixing model. A modified model will be discussed in a subsequent paper that provides quantitative agreement with all of the data sets presented here and is consistent with the known solution thermodynamics.

Acknowledgment. The authors thank B. P. Luo for assistance with the data sets required for the ternary refractive index calculation code and K. S. Carslaw for providing the source code for the analytic calculation of ternary solution compositions. We also appreciate the detailed and insightful comments provided by the reviewers of this manuscript. Support for this work was provided by the NASA Upper Atmospheres Research Program (UARP).

References and Notes

(1) Biermann, U. M.; Luo, B. P.; Peter, Th. *J. Phys. Chem. A* **2000**, *104*, 783−793.
(2) Molina, M. J. *Atmos. Environ.* **1991**, *25A* (11), 2535−2537.
(3) Toon, O. B.; Turco, R. P. *Sci. Amer.* **1991**, *264*, 68−74.

(4) Carslaw, K. S.; Peter, T.; Clegg, S. L. *Rev. Geophys.* **1997**, *35* (2), 125−154.

(5) Delnegro, J. R.; Fahey, D. W.; Donnelly, S. G.; Gao, R. S.; Keim, E. R.; Wamsley, R. C.; Woodbridge, E. L.; Dye, J. E.; Baumgardner, D.; Gandrud, B.; Wilson, J. C.; Jonsson, H. H.; Loewenstein, M.; Podolske, J. R.; Webster, C. R.; May, R. D.; Worsnop, D. R.; Tabazadeh, A.; Tolbert, M. A.; Keller, H. U.; Kelly, K. K.; Chan, K. R. *J. Geophys. Res.* **1997**, *102*, 13225−13282.

(6) Querry, M. R.; Waring, R. C.; Holland, W. E.; Earls, L. M.; Herrman, M. D.; Nijm, W. P.; Hale, G. M. *J. Opt. Soc. Am.* **1974**, *64*, 39−46.

(7) Remsberg, E. E.; Lavery, D.; Crawford, J. *J. Chem. Eng. Data* **1974**, *19*, 263−265.

(8) Pinkley, L. W.; Williams, D. *J. Opt. Soc. Am.* **1976**, *66*, 122−124.

(9) Palmer, K. F.; Williams, D. *Appl. Opt.* **1975**, *14*, 208−219.

(10) Tisdale, R. T.; Glandorf, D. L.; Tolbert, M. A.; Toon, O. B. *J. Geophys. Res.* **1998**, *D19*, 25353−25370.

(11) Niedziela, R. F.; Norman, M. L.; Miller, R. E.; Worsnop, D. R. *Geophys. Res. Lett.* **1998**, *25*, 4477−4480.

(12) Niedziela, R. F.; Norman, M. L.; DeForest, C. L.; Miller, R. E.; Worsnop, D. R. *J. Phys. Chem. A* **1999**, *103*, 8030−8040.

(13) Boone, T. L.; Fuller, K. A.; Downing, H. D. *J. Phys. Chem.* **1980**, *84*, 2666−2667.

(14) Querry, M. R.; Tyler, I. L. *J. Chem. Phys.* **1980**, *72*, 2495−2499.

(15) Toon, O. B.; Tolbert, M. A.; Koehler, B. G.; Middlebrook, A. M.; Jordan, J. *J. Geophys. Res.* **1994**, *99*, 25631−25654.

(16) Richwine, L. J.; Clapp, M. L.; Miller, R. E.; Worsnop, D. R. *Geophys. Res. Lett.* **1995**, *22*, 2625−2628.

(17) Niedziela, R. F.; Miller, R. E.; Worsnop, D. R. *J. Phys. Chem. A* **1998**, *102*, 6477−6484.

(18) Norman, M. L.; Qian, J.; Miller, R. E.; Worsnop, D. R. *J. Geophys. Res.* **1999**, *104*, 30571−30584.

(19) Adams, R. W.; Downing, H. D. *J. Opt. Soc. Am.* **1986**, *3*, 22−28.

(20) Luo, B. P.; Krieger, U. K.; Peter, T. *Geophys. Res. Lett.* **1996**, *23*, 3707−3710.

(21) Carslaw, K. S.; Luo, B.; Peter, T. *Geophys. Res. Lett.* **1995**, *22*, 1877−1880.

(22) Tabazadeh, A.; Turco, R. P.; Drdla, K.; Jacobson, M. Z.; Toon, O. B. *Geophys. Res. Lett.* **1994**, *21*, 1619−1622.

(23) Anthony, S. E.; Onasch, T. B.; Tisdale, R. T.; Disselkamp, R. S.; Tolbert, M. A. *J. Geophys. Res.* **1997**, *102*, 10777−10784.

(24) Carslaw, K. S.; Clegg, S. L.; Brimblecombe, P. *J. Phys. Chem.* **1995**, *99*, 11557−11574.

(25) Pueschel, R. F. *Composition, Chemistry, and Climate of the Atmosphere*; Van Nostrand Reinhold: New York, 1995; Chapter 5, pp 120−175.

(26) Clapp, M. L.; Worsnop, D. R.; Miller, R. E. *J. Phys. Chem.* **1995**, *99*, 6317−6326.

(27) Bohren, C. F.; Huffman, D. R. *Absorption and Scattering of Light by Small Particles*; Wiley: New York, 1983.